Research Article

Cancer Prevention Research

The Ashitaba (*Angelica keiskei*) Chalcones 4-hydroxyderricin and Xanthoangelol Suppress Melanomagenesis By Targeting BRAF and PI3K

Tianshun Zhang[1], Qiushi Wang[1], Mangaladoss Fredimoses[2], Ge Gao[1], Keke Wang[1,2], Hanyong Chen[1], Ting Wang[1,2], Naomi Oi[1], Tatyana A. Zykova[1], Kanamata Reddy[1], Ke Yao[1], Weiya Ma[1], Xiaoyu Chang[1], Mee-Hyun Lee[2], Moeez Ghani Rathore[1], Ann M. Bode[1], Hitoshi Ashida[3], Scott M. Lippman[4], and Zigang Dong[1,2]

Downloaded from http://aacrjournals.org/cancerpreventionresearch/article-pdf/11/10/607/1730510/607.pdf by guest on 23 May 2025

Abstract

Malignant melanoma is an aggressive tumor of the skin and still lacks effective preventive and therapeutic treatments. In melanoma, both the BRAF/MEK/ERK and PI3-K/AKT signaling pathways are constitutively activated through multiple mechanisms, which result in cell-cycle progression and prevention of apoptosis. Therefore, the development of novel strategies for targeting BRAF and PI3K are of utmost importance. In this study, we found that Ashitaba (*Angelica keiskei*) chalcones, 4-hydroxyderricin (4HD) and xanthoangelol (XAG), suppressed melanoma development by directly targeting both BRAFV600E and PI3K, which blocked the activation of downstream signaling. This led to the induction of G_1 phase cell-cycle arrest and apoptosis in melanoma cells. Importantly, 4HD or XAG dramatically attenuated tumor incidence and volume in the BRAF-activated *Pten*-deficient melanoma mouse model. Our findings suggest that 4HD and XAG are promising chemopreventive or potential therapeutic agents against melanomagenesis that act by targeting both BRAF and PI3K, providing hope for rapid clinical translation. *Cancer Prev Res; 11(10); 607–20. ©2018 AACR.*

Introduction

Melanoma is an aggressive tumor of the skin and strikes tens of thousands of people around the world each year (1). The American Cancer Society estimates that in the United States for 2018, about 91,270 new melanomas will be diagnosed and 9,320 people are expected to die of this disease. The number of cases is rising faster than any other type of solid cancer. However, effective preventive and therapeutic treatments are still insufficient and new drugs are desperately needed for clinical application.

The serial accumulation of molecular and genetic alterations is believed to occur in melanocytic transformation (2). Indeed, molecular alterations in many genes and metabolic pathways have been observed in melanoma. Over 50% of melanomas harbor activating V600E mutations in *BRAF* (3). This mutation is considered to be critical for the proliferation and survival of melanoma cells, through the activation of the RAF/MEK/ERKs MAPK pathway (4–6). Moreover, other mechanisms, for example, upregulation of PI3K/protein kinase B (AKT) signaling, increased expression of growth factor receptors on the cell membrane have been shown to be involved (7, 8). The PI3K/AKT pathway is one of the most important signaling networks in cancer. Accumulating evidence suggests that activation of this pathway plays a substantial and important role in melanoma (9–11). Aberrant expression and activity of the PI3K/AKT signaling cascade has been shown to increase the development of melanoma or melanomagenesis. The PI3K/AKT signaling pathway participates in the initiation, progression, and invasion of melanoma by inhibiting cell senescence and apoptosis pathways (12, 13). Therefore, in melanoma, the BRAF/MEK/ERKs and PI3K/AKT signaling

[1]The Hormel Institute, University of Minnesota, Austin, Minnesota. [2]The China-US (Henan) Hormel Cancer Institute, Zhengzhou, Henan, China. [3]Department of Agrobioscience, Graduate School of Agricultural Science, Kobe University, Nada-ku, Kobe, Japan. [4]University of California San Diego Health Science.

Note: Supplementary data for this article are available at Cancer Prevention Research Online (http://cancerprevres.aacrjournals.org/).

T. Zhang and Q. Wang contributed equally to this article.

Corresponding Authors: Scott M. Lippman, University of California, San Diego, Moores Cancer Center, La Jolla, CA 92093; Phone: 858-822-1222; E-mail: slippman@ucsd.edu; and Zigang Dong, The Hormel Institute, University of Minnesota, 801 16th Ave NE, Austin, MN 55912. Phone: 507-437-9600; Fax: 507-437-9606; E-mail: zgdong@hi.umn.edu

doi: 10.1158/1940-6207.CAPR-18-0092

©2018 American Association for Cancer Research.

pathways play a vital role in fundamental signal transduction and mediation of many of the physiologic processes involved. Strategies targeting both BRAF and PI3K should be a promising approach to develop clinically effective therapies for the treatment of melanoma.

The chalcones, 4-hydroxyderricin (4HD) and xanthoangelol (XAG), are considered to be major active compounds of the Japanese herb Ashitaba exerting various biofunctions such as anti-inflammatory effects, prevention of obesity and antidiabetic activities (14–16). However, the effects of either compound on skin carcinogenesis are still unknown. In this study, we demonstrated that 4HD or XAG suppressed melanomagenesis. We identified two target proteins of 4HD and XAG and demonstrated their effects on downstream signaling cascades. Furthermore, we conducted experiments to show the effect of 4HD or XAG on cell cycle and apoptosis in melanoma cells. Finally, we demonstrated the effects of 4HD or XAG in the BRAFV600E/PTEN-null mouse model, which expresses highly active BRAF/MEK/ERKs and PI3K/AKT pathways (17).

Materials and Methods

Cell culture

SK-MEL-28, SK-MEL-5, and SK-MEL-31 cells were purchased from ATCC and normal human epidermal melanocytes (NHEM) were purchased from PromoCell. The cells were routinely screened to confirm *Mycoplasma*-negative status and to verify the identity of the cells by short tandem repeat (STR) profiling before being frozen. Each vial was thawed and maintained in culture for a maximum of 2 months. Enough frozen vials of each cell line were available to ensure that all cell-based experiments were conducted on cells that had been tested and in culture for 2 months or less. All cells were cultured in Eagle's MEM with 10% FBS and 1% antibiotics. Cell culture medium, gentamicin, penicillin, and L-glutamine were all obtained from Invitrogen. FBS was from Gemini Bio-Products. NHEM cells were cultured in melanocyte growth medium with Supplement Mix (PromoCell). All cell culture conditions were performed following ATCC and PromoCell protocols.

Reagents and antibodies

4HD and XAG were extracted and purified from Ashitaba (*Angelica keiskei*) powder that was provided by Japan Bio Science Laboratory Co., Ltd. The powder was mixed with water and then extracted with ethyl acetate (EtOAc; 1.5 L × 3 times) under reflux. The combined EtOAc extracts were concentrated to give a brownish yellow colored viscous mass (48.245 g), which was chromatographed on a silica gel column. The column was eluted with hexane/EtOAc in a linear gradient (90:10, 80:20, 50:50, 25:75), followed by $CHCl_3$/MeOH in a linear gradient (90:10, 80:20, 70:30, 60:40, 0:100) to obtain 6 fractions (Fr. 1–6) on the basis of thin-layer chromatography (TLC) profiles. Fr. 3 (6.385 g) was rechromatographed on a silica column with $CHCl_3$/MeOH (100:1 to 30:1) and RP-18 with 80% MeOH to purify 4HD (3.163 g). Fr. 4 (5.873 g) was produced following a similar elution procedure as for Fr. 3 and washed on a LH-20 Sephadex column with MeOH to purify XAG (2.989 g). Then the 4HD and XAG were identified by NMR spectra (Supplementary Fig. S1A and S1B). The NMR spectra were obtained on a Bruker AVANCE-500 spectrometer (Bruker) with tetramethylsilane (TMS) as the internal standard. High-resolution electrospray ionization mass spectrometry (HRESIMS) was performed on the Q-T of Micro mass spectrometer (Waters). The silica gel (100–200 and 200–300 mesh) and Sephadex LH-20 for column chromatography were purchased from Qingdao Marine Chemical Group Co. and GE Healthcare, respectively. All solvents used were of analytical grade (Tianjin Fuyu Chemical and Industry Factory, Tianjin, China).

Tris, NaCl, and SDS for molecular biology and buffer preparation were purchased from Sigma-Aldrich. Antibodies to detect actin (SC-47778), cyclin D1 (SC-8396), Bcl-2 (SC-7382), GAPDH (SC-25778), and BRAF (SC-166) were from Santa Cruz Biotechnology, Inc.. Unless otherwise specified, the antibodies p-MEK (#9121), MEK (#9122), p-ERKs (#9101), ERKs (#9102), p-AKT (Ser473) (#9271), AKT (#4691), PI3-K (#4249), cleaved PARP (#9541), PARP (#9542), cleaved caspase-3 (#9661), and caspase-3 (#9662) were from Cell Signaling Technology.

Pull-down assays

4HD or XAG (2.5 mg) was coupled to CNBr-activated Sepharose 4B (GE Healthcare Biosciences) matrix beads (0.5 g) in 0.5 mol/L NaCl and 40% DMSO (pH 8.3) overnight at 4°C, according to the manufacturer's instructions. SK-MEL28 cell lysates (500 μg) were mixed with 4HD or XAG-conjugated Sepharose 4B beads or with Sepharose 4B beads alone as a control in reaction buffer (50 mmol/L Tris-HCl pH 7.5, 5 mmol/L EDTA, 150 mmol/L NaCl, 1 mmol/L dithiothreitol (DTT), 0.01% NP-40, 2 μg/mL BSA, 0.02 mmol/L phenylmethylsulfonyl fluoride (PMSF), and 1 × protease inhibitor cocktail). After gentle rocking at 4°C overnight, the beads were washed 5 times with buffer (50 mmol/L Tris-HCl pH 7.5, 5 mmol/L EDTA, 150 mmol/L NaCl, 1 mmol/L DTT, 0.01% NP-40, and 0.02 mmol/L PMSF). Binding was examined by Western blotting.

In vitro kinase assay

An *in vitro* BRAF activation kinase assay was conducted according to the instructions provided by Millipore. Briefly, reactions were performed in the presence of 10 μCi [γ^{32}P] ATP with active MEK1 (1 μg), 4HD, or XAG (0, 5, 10, or 20 μmol/L) in 40 μL of reaction buffer (40 mmol/L MOPS/NaOH pH 7.0, 1 mmol/L EDTA, 10 mmol/L $MnCl_2$, and 0.8 mol/L ammonium sulphate) at 30°C for 30 minutes. Reactions were stopped by adding 10-μL protein loading

Downloaded from http://aacrjournals.org/cancerpreventionresearch/article-pdf/11/10/607/1730510/607.pdf by guest on 23 May 2025

buffer and the mixture was separated by SDS-PAGE. The relative amounts of incorporated radioactivity were assessed by autoradiography.

An *in vitro* PI3K assay was conducted at 30°C for 10 minutes with 100 ng of PI3K and different doses of 4HD, XAG, or LY294002. Each sample was mixed with 20 μL of 0.5 mg/mL phosphatidylinositol as substrate at room temperature for 5 minutes and then incubated an additional 10 minutes at 30°C with reaction buffer [0.25 mmol/L ATP containing 10 μCi [γ-^{32}P]ATP, 10 mmol/L Tris-HCl (pH 7.6), and 60 mmol/L $MgCl_2$]. The reaction was stopped by adding 15 μL of 4 N HCl and 130 μL of chloroform: methanol (1:1). After vortexing and fractionation, the lower chloroform phase was spotted onto a silica gel plate (EMD Millipore Corp.) that was preheated at 110°C for 1 hour. The resulting radiolabeled spots were visualized by autoradiography.

In vitro CDK4 and CDK6 activation kinase assays were conducted according to the instructions provided by SignalChem. Briefly, reactions were performed in the presence of 10 μCi [γ^{32}P] ATP with 2 μg Rb-C fusion protein (701–928 amino acid) from Cell Signaling Technology, 4HD, or XAG (0, 10, or 20 μmol/L) in reaction buffer at 30°C for 30 minutes. Reactions were stopped by adding 10-μL protein loading buffer and the mixture was separated by SDS-PAGE. The relative amounts of incorporated radioactivity were assessed by autoradiography.

Molecular modeling

The computer modeling of 4HD or XAG with BRAFV600E and PI3K was performed using the Schrödinger Suite 2015 software programs (18). The BRAFV600E and PI3K crystal structures were prepared under the standard procedure of the Protein Preparation Wizard in Schrödinger Suite 2015. Hydrogen atoms were added consistent with a pH of 7 and all water molecules were removed. The ATP-binding site–based receptor grid was generated for docking. 4HD or XAG was prepared using the LigPrep program (Schrödinger) and the lowest energy conformations for docking were determined by using default parameters under the extra precision (XP) mode and the program Glide. The protein-ligand docking analysis was conducted using the induced fit docking program of Schrödinger, which can provide ligand-binding flexibility with binding pocket residues.

MTS assay

SK-MEL-5, SK-MEL-28, and SK-MEL-31 cells (1×10^3 cells/well) were seeded into 96-well plates in 100 μL of 10% FBS/Eagle MEM. The cells were treated with 4HD or XAG. After incubation for 1, 2, 3, or 4 days, NHEM cells (1×10^4 cells/well) were seeded into 96-well plates for determining cytotoxicity. After an overnight incubation, cells were treated with different concentrations (5, 10, or 20 μmol/L) of 4HD or XAG or vehicle control and incubated for 1 or 2 days. Then 20 μL of the CellTiter 96 Aqueous One Solution (Promega) were added to each well and cells were then incubated for an additional 1 hour at 37°C. Absorbance was measured at an optical density of 492 and 690 nm using the Thermo Multiskan plate-reader (Thermo Fisher Scientific).

Anchorage-independent cell growth assay

Cells (8×10^3/well) were seeded into 6-well plates with 0.3% basal medium Eagle agar containing 10% FBS and different concentrations of 4HD or XAG and then cultured for 2 weeks. Colonies were scored under a microscope using the Image-Pro PLUS (v6.) computer software program (Media Cybernetics).

Western blot analysis

Equal amounts of protein were determined using a protein assay kit (Bio-Rad Laboratories). Lysates were resolved by SDS-PAGE and then transferred onto polyvinylidene difluoride membranes (EMD Millipore Corp.) and blocked with 5% nonfat milk for 1 hour at room temperature. Blots were probed with appropriate primary antibodies (1:1,000) overnight at 4°C and followed by incubation with a horseradish peroxidase (HRP)-conjugated secondary antibody (1:5,000) for hybridization. Protein bands were visualized with a chemiluminescence reagent (GE Healthcare Biosciences).

Cell-cycle analysis

SK-MEL-28 cell cycle was evaluated using a published method (19). In brief, after arresting the cells in the G_0 phase, the cells were treated with various concentrations of 4HD, XAG, or vehicle control for 6, 12, 18, 24, or 48 hours. After fixing with ethanol, cells were stained with propidium iodide and the cell-cycle phase was determined by flow cytometry.

Flow cytometry for analysis of apoptosis

For analysis of apoptosis, SK-MEL-28 cells (2.5×10^5/well) were seeded into 60-mm dishes overnight and then the cells were treated with 4HD or XAG for 72 hours. Cells were trypsinized and washed twice with cold PBS and then resuspended with PBS and incubated for 5 minutes at room temperature with Annexin V-FITC plus propidium iodide. Cells were analyzed using a FACSCalibur flow cytometer (BD Biosciences).

Animal studies

All animal studies were performed following guidelines approved by the University of Minnesota Institutional Animal Care and Use Committee (Minneapolis, MN), protocol approval number (1501-32220A).

BRAF V600E/PTEN-null mice (B6.Cg-*Braf*^{tm1Mmcm} *Pten*^{tm1Hwu} Tg(Tyr-cre/ERT2)13Bos/BosJ) were purchased from The Jackson Laboratory. The mice were housed and bred in a virus and antigen-free room. Mice were genotyped by standard PCR analysis according to the

Downloaded from http://aacrjournals.org/cancerpreventionresearch/article-pdf/11/10/607/1730510/607.pdf by guest on 23 May 2025

Jackson Laboratory genotyping protocol. Mice with the BRAFV600E mutation heterozygote and PTEN loss with Cre were used in this study. For localized melanoma induction on the dorsal skin, adult (6–8 weeks of age) mice were treated topically with 2.5 μL of 1.9 mg/mL (5 mmol/L) 4-hydroxytamoxifen (4-HT; Sigma-Aldrich, H6278) for 3 days. 4HD and XAG were dissolved in PBS with 2.5% dimethyl sulfoxide (DMSO), 5% polyethylene glycol 400 (PGE 400), and 5% Tween 80. The compounds were administered to mice by oral gavage at a dose of 10 or 50 mg/kg body weight. The relevant solvent was administered to control animals in the melanoma prevention studies. For the early treatment study, the compounds or solvent were administered to the mice daily after 4-HT treatment. For the late treatment study, the compounds or solvent were administered to the mice daily beginning at day 23, when the animals had readily measurable melanoma lesions.

IHC analysis of mouse melanoma tissues

A Vectastain Elite ABC Kit obtained from Vector Laboratories was used for IHC staining according to the protocol recommended by the manufacturer. Mouse melanoma tissues were fixed in 10% buffered formalin phosphate (Fisher Chemical) and embedded in paraffin for examination. Sections were stained and analyzed by IHC. Briefly, all specimens were baked at 60°C for 2 hours, deparaffinized, and rehydrated. To expose antigens, samples were unmasked by submerging each into boiling sodium citrate buffer (10 mmol/L, pH 6.0) for 10 minutes, and then treated with 3% H_2O_2 for 10 minutes. The slides were blocked with 50% goat serum albumin in 1× PBS in a humidified chamber for 1 hour at room temperature. Then, the mouse tissue sections were hybridized with PCNA (1:3,000), cyclin D1 (1:75), or Bcl-2 (1:50) antibody at 4°C in a humidified chamber overnight. The slides were washed and hybridized with the secondary antibody from Vector Laboratories (anti-rabbit 1:200 or anti-mouse 1:200) for 1 hour at room temperature. Slides were stained using the Vectastain Elite ABC Kit (Vector Laboratories, Inc.).

Statistical analysis

All quantitative data are expressed as mean values ± SD or standard error (SE) of at least three independent experiments. Significant differences were determined by a Student *t* test or one-way ANOVA. A probability value of $P < 0.05$ was used as the criterion for statistical significance.

Results

4HD or XAG binds to target kinases at the ATP-binding pocket

Induced fit docking was conducted to determine whether 4HD or XAG could bind with BRAFV600E or PI3K. The structure of 4HD (left) or XAG (right) is shown in Fig. 1A. The results indicated that 4HD or XAG formed interactions within the ATP-binding pocket of BRAFV600E and PI3K (Fig. 1B and C; Supplementary Fig. S2A and S2B). For the binding of 4HD with BRAFV600E, the carbonyl oxygen of 4HD interacts with the residue CYS532 hydrogen of BRAFV600E and the distance is 2.06 Å. For the binding of XAG with BRAFV600E, the 4′-hydroxy oxygen of XAG interacts with the residue CYS532 hydrogen of BRAFV600E and the distance is 1.78 Å. The 4′-hydroxy hydrogen of XAG interacts with the residue CYS532 oxygen of BRAFV600E and the distance is 1.90 Å. The 4-hydroxy hydrogen of XAG interacts with the side chain GLU501 oxygen of BRAFV600E and the distance is 2.84 Å. For 4HD binding with PI3K, the 2′-hydroxy hydrogen of 4HD interacts with the residue VAL851 oxygen of PI3K and the distance is 2.19 Å. The 2′-hydroxy oxygen of 4HD interacts with the residue VAL851 hydrogen of PI3-K and the distance is 2.10 Å. The carbonyl oxygen of 4HD interacts with the residue VAL851 hydrogen and the distance is 2.63 Å. For XAG binding with PI3K, the 2′-hydroxy hydrogen of XAG interacts with the residue VAL851 oxygen and the distance is 2.03 Å. The 2′-hydroxy oxygen of XAG interacts with the residue VAL851 hydrogen and the distance is 1.97 Å. The carbonyl oxygen of XAG interacts with the residue VAL851 hydrogen and the distance is 2.80 Å. The 4-hydroxy oxygen of XAG interacts with the side chain LYS802 hydrogen of PI3K and the distance is 3.03 Å and the 4-hydroxy hydrogen of XAG interacts with the side chain ASP oxygen of PI3K and the distance is 2.82 Å. Furthermore, we observed *ex vivo* binding between 4HD or XAG and BRAF and PI3K (p110) in SK-MEL28 cell lysates (Fig. 1D). Taken together, our data indicated that 4HD or XAG interacts with BRAFV600E and PI3K.

4HD or XAG suppresses BRAF and PI3K kinase activity

On the basis of the results of the computer computational modeling and the *ex vivo* binding assay, we predicted that 4HD or XAG is a potential inhibitor of BRAFV600E and PI3-K. To elucidate the mechanisms and the activity of 4HD and XAG, we conducted a kinase-profiling assay to determine the effect of each compound on the *in vitro* kinase activity of BRAFV600E, PI3K, and other candidate kinases, which included the previously predicted targeted kinases. Kinase profiling was performed by Millipore's KinaseProfiler based on the protocols provided by Millipore. Data are presented as percentage of kinase activity remaining after treatment with 4HD or XAG (Supplementary Table S1). At a concentration of 10 μmol/L, 4HD or XAG inhibited the activity of BRAFV600E and the activity of PI3K. However, 4HD or XAG, at the same concentration, had little effect on the activity of ERKs, MEK, or other kinases. We also found that 4HD or XAG did not affect CDK4 and CDK6 activation (Supplementary Fig. S3A and S3B). We then conducted *in vitro* kinase assays to verify the kinase profiling results. The density of specific bands was

Downloaded from http://aacrjournals.org/cancerpreventionresearch/article-pdf/11/10/607/1730510/607.pdf by guest on 23 May 2025

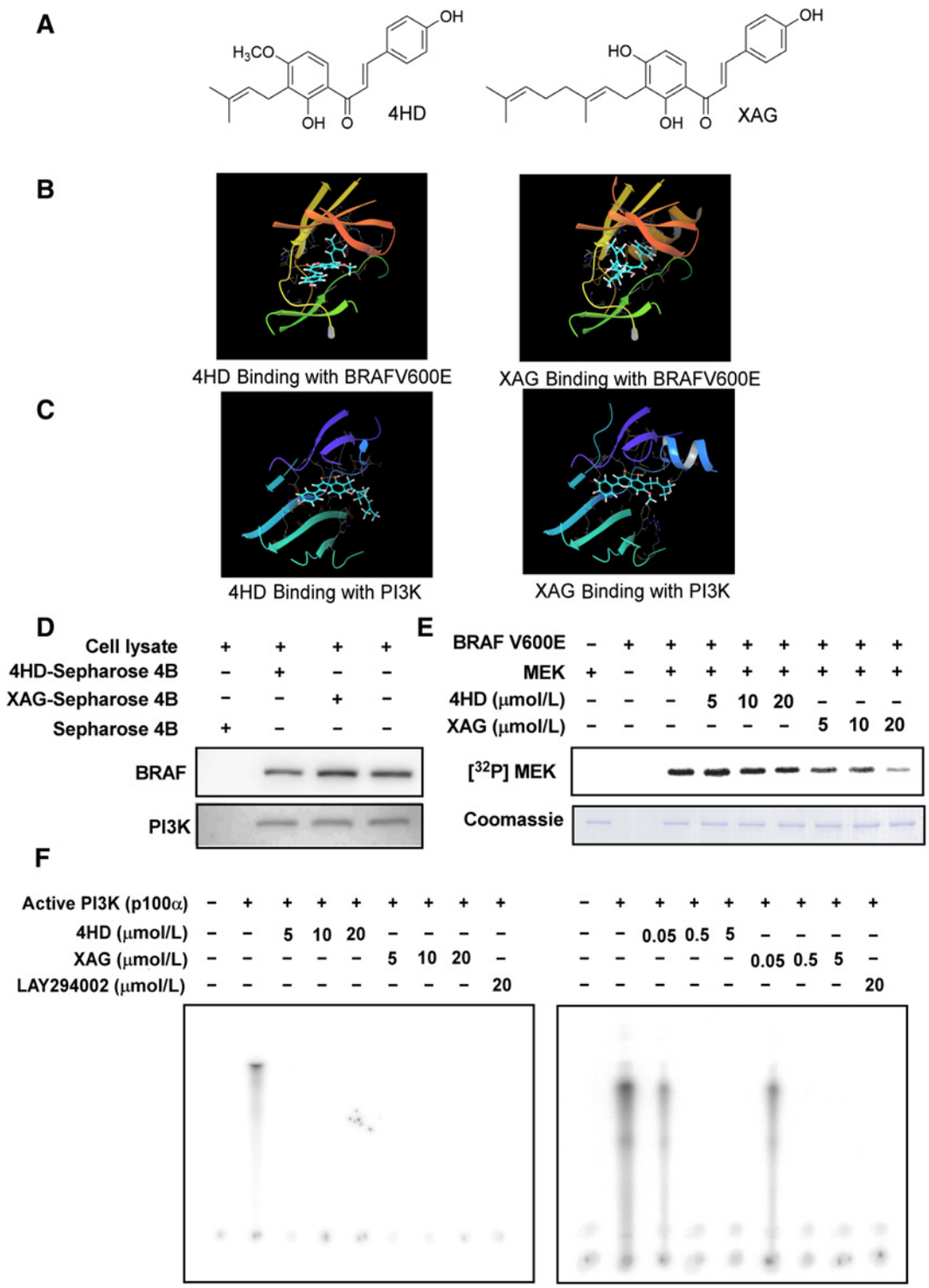

Figure 1.

4HD or XAG binds to and effectively suppresses BRAFV600E and PI3K activity. **A,** The structures of 4HD and XAG. Computer docking model for 4HD or XAG and target kinases, including BRAFV600E (**B**) and PI3K (**C**). The binding was further confirmed by an *in vitro* binding assay. **D,** SK-MEL-28 cell lysates (500 μg) were incubated with 4HD- or XAG-conjugated Sepharose 4B beads or Sepharose 4B beads alone and the pulled-down proteins were analyzed by Western blotting. **E,** 4HD or XAG inhibits BRAFV600E activity *in vitro*. Reactions were performed in the presence of 10 μCi [γ^{32}P] ATP with active MEK1, 4HD, or XAG (0, 5, 10, or 20 μmol/L) in 40 μL of reaction buffer at 30°C for 30 minutes. **F,** 4HD or XAG inhibits PI3-K kinase activity *in vitro*. Active kinase PI3K (p110) and different doses of 4HD, XAG, or LY294002, a PI3K kinase inhibitor, were mixed with the substrate phosphatidylinositol and then incubated with a [γ^{32}P] ATP mixture. The relative amounts of incorporated radioactivity were visualized by autoradiography.

Downloaded from http://aacrjournals.org/cancerpreventionresearch/article-pdf/11/10/607/1730510/607.pdf by guest on 23 May 2025

calculated using the Image J analysis software program. The results showed that 4HD suppressed BRAFV600E activation by 17.4% ± 4.1% at 20 μmol/L, whereas XAG strongly suppressed BRAFV600E activation in a dose-dependent manner. XAG at 5, 10, or 20 μmol/L reduced BRAFV600E kinase activity by 23.7% ± 8.5%, 50.6% ± 9.1%, or 81.4% ± 6.4%, respectively (Fig. 1E). Moreover, either 4HD or XAG at 0.05 μmol/L strongly suppressed PI3K (p100/p85) activity by 42.5% and 46.6% (Fig. 1F), respectively. Taken together, these results indicate that BRAFV600E and PI3-K (p110/85) are effective targets of 4HD and XAG.

4HD or XAG suppress human melanoma cell colony formation and proliferation

On the basis of the previous results, we then determined whether 4HD or XAG had any effect on the anchorage-independent growth and proliferation of human melanoma cells. To determine whether 4HD or XAG exerted any cytotoxic effects against normal melanocytes, NHEM cells were treated with different concentrations of 4HD or XAG for 1 or 2 days. The results showed that 4HD or XAG had no cytotoxicity at concentrations less than 20 μmol/L (Supplementary Fig. S4A and S4B). Next, we examined the effects of 4HD or XAG on melanoma SK-MEL-5 and SK-MEL-28 cell colony formation and proliferation. The results showed that either 4HD or XAG inhibited SK-MEL-28 and SK-MEL-5 melanoma cell colony formation in soft agar and proliferation in MTS assay in a dose-dependent manner (Fig. 2A and B). These results indicate that 4HD or XAG can effectively inhibit melanoma cell growth. In addition, we examined the effect of 4HD and XAG on proliferation in SK-MEL-31 melanoma cells, which harbors wild-type BRAF (Supplementary Fig. S4C). The results showed that 4HD only at 20 μmol/L significantly inhibited proliferation of SK-MEL-31 cells, whereas XAG at 10 or 20 μmol/L significantly inhibited proliferation of SK-MEL-31 cells. As low as 5 μmol/L, 4HD or XAG significantly inhibited growth of SK-MEL-5 and SK-MEL-28 cells. These results indicated that 4HD and XAG were less effective on inhibiting growth of wild-type BRAF cells (SK-MEL-31) compared with BRAFV600E–mutant cells (SK-MEL-5 and SK-MEL-28), which suggested selectivity.

4HD or XAG suppresses the BRAF and PI3K downstream kinase signaling pathways in melanoma cells

We have shown that 4HD or XAG can inhibit BRAFV600E and PI3K activation. Here, we examined the effect of 4HD or XAG on the downstream signaling of BRAFV600E and PI3K in SK-MEL-28 cells, which express the BRAFV600E mutation. Treatment of SK-MEL-28 cells with either 4HD or XAG led to a substantial inhibition of phosphorylated AKT (Ser473), downstream of PI3-K in a dose-dependent manner. In addition, 4HD slightly suppressed the phosphorylation of MEK1/2 and ERK1/2, which are downstream of BRAF. Notably, XAG also decreased the phosphorylation of MEK1/2 and ERK1/2 in a dose-dependent manner (Fig. 2C). These data indicate that either 4HD or XAG can suppress melanoma cell growth by inhibiting the activation of BRAF/MEK/ERKs and PI3K/AKT signaling pathways.

4HD or XAG induces G_0–G_1 cell-cycle arrest in melanoma cells

To determine whether 4HD or XAG can affect cell-cycle progression, the SK-MEL-28 melanoma cells were first cultured with 4HD or XAG (15 μmol/L) for 6, 12, 18, 24, or 48 hours and then stained with propidium iodide. Results showed that either 4HD or XAG induced G_0–G_1 cell-cycle arrest, as compared with untreated controls (Fig. 3A; Supplementary Fig. S5A). Notably, XAG strongly induced G_0–G_1 arrest as compared with the control. Moreover, the treatment of SK-MEL-28 cells with either 4HD or XAG led to G_0–G_1 cell-cycle arrest in a dose-dependent manner at 18 hours (Fig. 3B; Supplementary Fig. S5B). Furthermore, 4HD or XAG decreased cyclin D1 expression in a dose-dependent manner, which was associated with G_0–G_1 cell-cycle arrest in melanoma cells (Fig. 3C). Overall, these results indicate that the inhibition of cell-cycle progression plays a role in 4HD or XAG attenuation of melanoma cell growth.

4HD or XAG induces apoptosis in melanoma cells

Annexin V staining was used to determine the effect of 4HD or XAG on apoptosis in SK-MEL-28 cells (Fig. 4). Results showed that apoptosis was induced in a dose-dependent manner after exposure to 4HD or XAG (Fig. 4A and B). The cleavage of PARP and caspase-3 facilitates cellular disassembly and Bcl-2 is an important antiapoptotic protein. Consistent with the results of Annexin V staining, our Western blot results demonstrated that in the presence of 4HD or XAG, the levels of cleaved PARP or caspase-3 were increased, whereas the levels of Bcl-2 were decreased in melanoma cells (Fig. 4C). All these data suggest that 4HD or XAG treatment potently induces apoptosis in human melanoma cells.

Effect of 4HD or XAG on melanomagenesis in the BRAFV600E-mutant and PTEN-loss mouse model

To determine whether treatment with either 4HD or XAG has a preventive effect on melanomagenesis *in vivo*, experiments were conducted in a mouse model. BRAFV600E-mutant and PTEN-loss mice were treated topically on the back with 4-HT for 3 days. On day 4, mice were randomly assigned to groups as follows: (i) mice administered 4HD (10 mg/kg, $n = 10$; or 50 mg/kg, $n = 10$); (ii) XAG (10 mg/kg, $n = 10$; or 50 mg/kg, $n = 10$), or (iii) solvent control ($n = 10$) daily (Fig. 5A). The animals were monitored daily and tumor volume and body weight were measured once a week. Our results showed that 4HD or XAG strongly suppressed the occurrence and development

Downloaded from http://aacrjournals.org/cancerpreventionresearch/article-pdf/11/10/607/1730510/607.pdf by guest on 23 May 2025

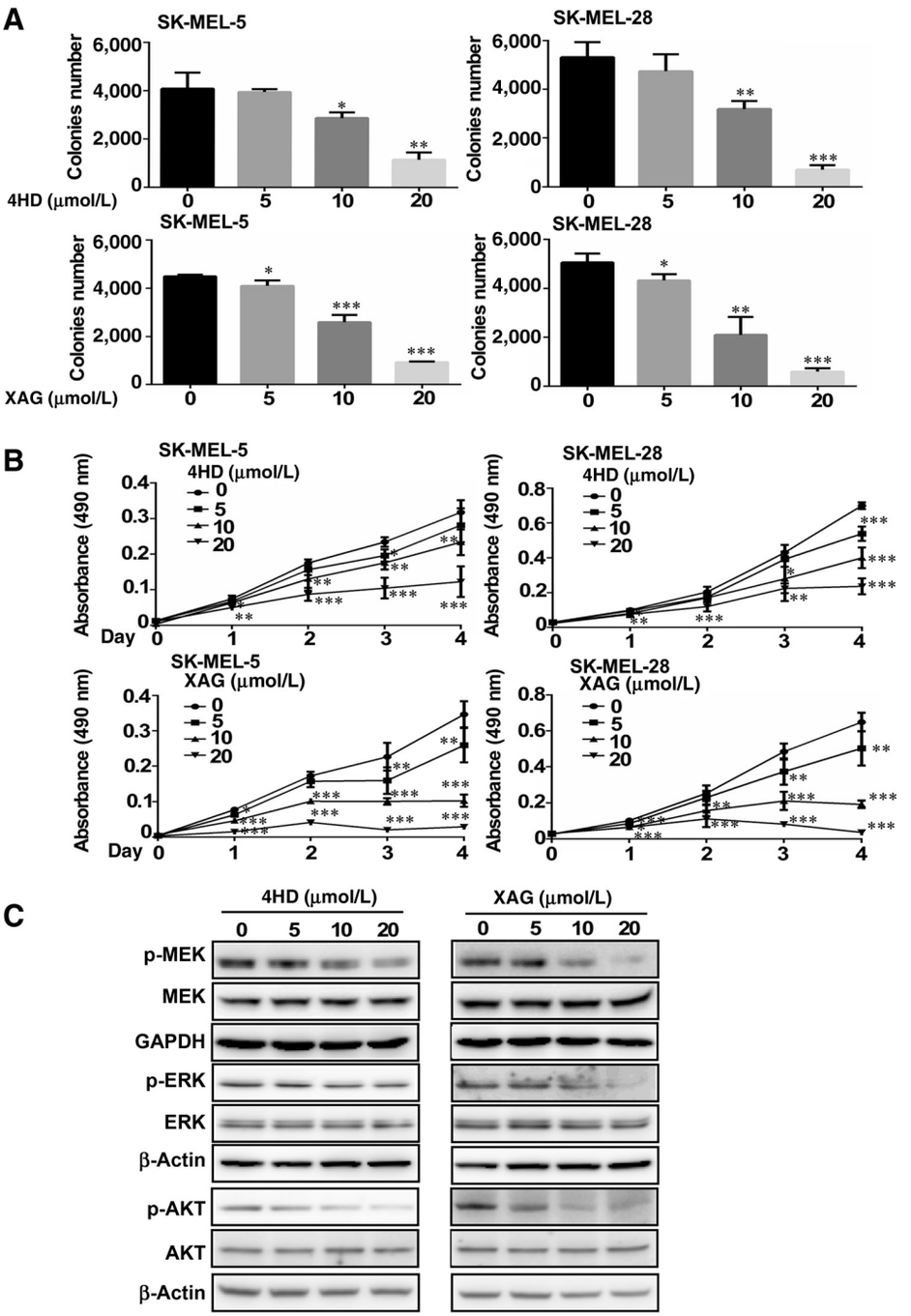

Figure 2.

Effects of 4HD or XAG on growth and target protein expression levels in melanoma cells. **A,** 4HD or XAG inhibits anchorage-independent cell growth. Cells (8×10^3/well) were seeded into 6-well plates with 0.3% basal medium Eagle agar containing 10% FBS and different concentrations of 4HD or XAG and then cultured for 2 weeks. Colonies were scored under a microscope using the ImageJ software program. **B,** 4HD or XAG inhibits proliferation of melanoma cells. SK-MEL-5 and SK-MEL-28 cells (1×10^3 cells/well) were seeded into 96-well plates. The cells were treated with 4HD or XAG. After incubation for 1, 2, 3, or 4 days, viability was estimated using the MTS assay as described in Materials and Methods. **C,** SK-MEL-28 (70–80% confluent) melanoma cells were incubated with the indicated concentrations of 4HD or XAG for 24 hours and then the expression of target proteins was determined by Western blotting. Data are represented as mean values ±SD as determined from three independent experiments. The asterisks indicate a significant decrease compared with untreated control cells (*, $P < 0.05$; **, $P < 0.01$; ***, $P < 0.001$).

of melanoma (Fig. 5B; Supplementary Fig. S6). Either 4HD or XAG significantly reduced the volume of melanoma tissue and led to significantly decreased tumor weight at the endpoint of the experiment. Notably, 4HD treatment decreased melanoma volume by 54% (10 mg/kg) and 97% (50 mg/kg), respectively. Moreover, XAG treatment decreased melanoma volume by 68% (10 mg/kg) and 97% (50 mg/kg), respectively. On the basis of our findings, 4HD or XAG attenuated activation of BRAFV600E and PI3K. We also determined the levels of phosphorylated ERK1/2 and AKT (Ser473), which are downstream of BRAFV600E and PI3K. We found that these agents markedly inhibited the phosphorylation of ERK1/2 and AKT (Fig. 5C). This was associated with the reduced expression of PCNA, cyclin D1, and Bcl-2, which are associated with melanoma cell proliferation and apoptosis (Fig. 5D).

To determine whether treatment with either 4HD or XAG had inhibitory effects on melanomagenesis when tumors

Downloaded from http://aacrjournals.org/cancerpreventionresearch/article-pdf/11/10/607/1730510/607.pdf by guest on 23 May 2025

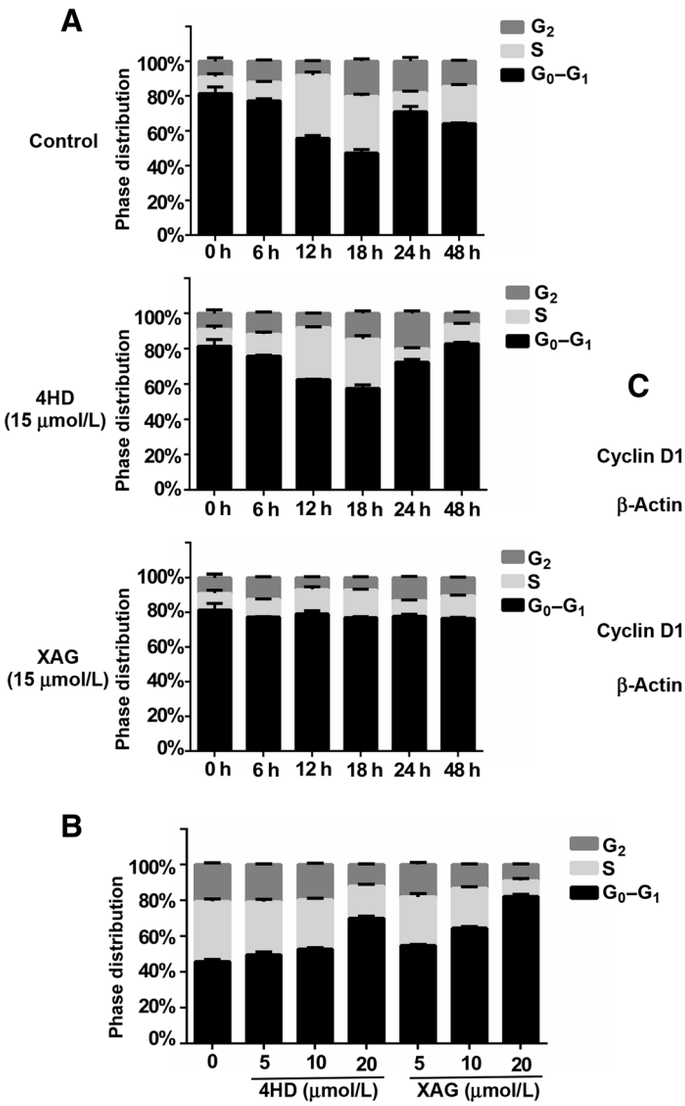

Figure 3.
4HD or XAG induces G_1 arrest in melanoma cells. SK-MEL-28 melanoma cells (2.5×10^4/well) were cultured in 60-mm plates and then synchronized in the G_0-phase by serum deprivation. **A,** The cells were treated with 15 μmol/L 4HD or XAG or vehicle control for 6, 12, 18, 24, or 48 hours. **B,** The cells were treated with various concentrations of 4HD, XAG, or vehicle control for 18 hours. After fixing with ethanol, cells were stained with propidium iodide and the cell-cycle phase was determined by flow cytometry. **C,** To determine the effect of 4HD or XAG on G_1 phase–associated cyclin D1 protein expression, Western blotting was performed using cyclin D1 and β-actin antibodies.

were measurable, mice were treated topically on the dorsal surface with 4-HT for 3 days. After 23 days, when tumors were observed, the mice were randomly assigned to groups as follows: (i) administered 4HD (10 mg/kg, $n = 10$; or 50 mg/kg, $n = 10$); (ii) XAG (10 mg/kg, $n = 10$; or 50 mg/kg, $n = 10$), or (iii) solvent control ($n = 10$) daily (Fig. 6A). Our results showed that 4HD or XAG at 10 mg/kg body weight significantly reduced the volume of melanoma tissue by 43% and 72%, respectively. At 50 mg/kg body weight, tumor volume was significantly reduced by 82% and 91%, respectively. Similar inhibitory effects were observed on final tumor weight (Fig. 6B; Supplementary Fig. S7). We found that these agents markedly inhibited tumor growth. In addition, our results also showed that 4HD or XAG clearly inhibited the phosphorylation levels of ERK1/2 and AKT in a dose-dependent manner (Fig. 6C), which resulted in reduction of the expression of PCNA, cyclin D1, and Bcl-2 (Fig. 6D).

Discussion

Over the past few decades, melanoma has been on the rise around the world. According to the World Health Organization (WHO), 132,000 cases of melanoma occur globally each year. Targeted therapy that depends on activated oncogenes and the downstream signaling cascades has emerged as an impressive approach for advanced melanoma. In this study, we report that the natural compounds, 4HD or XAG (Fig. 1A), effectively suppress melanomagenesis by targeting BRAFV600E and PI3K.

Computer simulation and computational modeling are useful tools for analyzing and increasing our knowledge of complex interactions, with the aim of identifying and elucidating a drug's molecular target(s). Using this method, we found that the Ashitaba (*Angelica keiskei*) chalcones, 4HD and XAG, are potential inhibitors against BRAFV600E and PI3K (Fig. 1B–D). Kinase activity assays showed that

Downloaded from http://aacrjournals.org/cancerpreventionresearch/article-pdf/11/10/607/1730510/607.pdf by guest on 23 May 2025

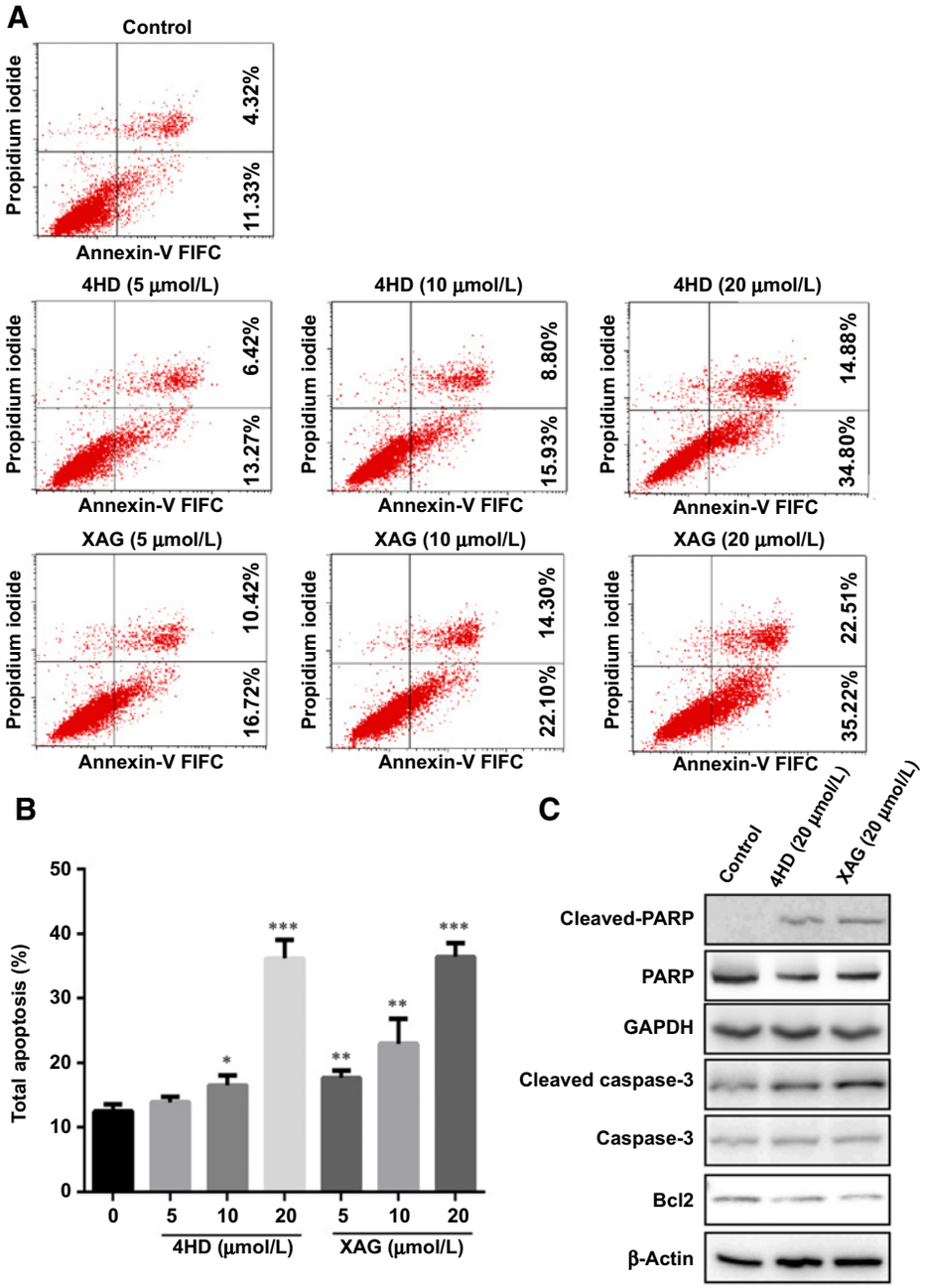

Figure 4.

4HD or XAG induces apoptosis in melanoma cells. **A** and **B,** SK-MEL-28 cells (2.5×10^5/well) were incubated with 4HD or XAG (5, 10, or 20 μmol/L), or vehicle control for 72 hours. Cells were collected and apoptosis was detected using flow cytometry and Annexin V staining. Data are represented as mean values ±SD as determined from three independent experiments and the asterisks indicate a significant decrease compared with untreated control cells (*, $P < 0.05$; **, $P < 0.01$; ***, $P < 0.001$). **C,** The cells were incubated with 20 μmol/L 4HD or XAG or vehicle control for 72 hours, then the effect of 4HD or XAG on apoptosis-associated protein expression was determined by Western blotting.

either 4HD or XAG suppresses the activity of BRAFV600E and PI3K, with the subsequent reduction of phosphorylation of downstream kinases, MEKs, ERKs, and AKT (Figs. 1E and F and 4). These findings indicate that 4HD and XAG are inhibitors of both BRAFV600E and PI3-K. Over 50% of melanomas harbor activating V600E mutations in *BRAF* (3). In the clinic, selective inhibitors have shown marked tumor regression and improved survival of late-stage BRAF-mutated melanoma and BRAFV600E-mutant metastatic melanoma patients (20–23). For a short period following treatment, the patients have an improved quality of life. However, most patients relapse with lethal drug-resistant disease, eventually resulting in death (24). Combining BRAF inhibition with MEK inhibition leads to improved progression-free survival as compared with BRAF inhibition alone (25, 26). However, not all melanomas express the mutated BRAF protein, and not all melanomas with mutant BRAF are responsive to these targeted therapies. Apparently, merely inhibiting the BRAF/MEK/ERKs signaling pathway is not enough to completely suppress melanomagenesis. Recently, several reports indicate that the PI3K/AKT pathway activation is

Downloaded from http://aacrjournals.org/cancerpreventionresearch/article-pdf/11/10/607/1730510/607.pdf by guest on 23 May 2025

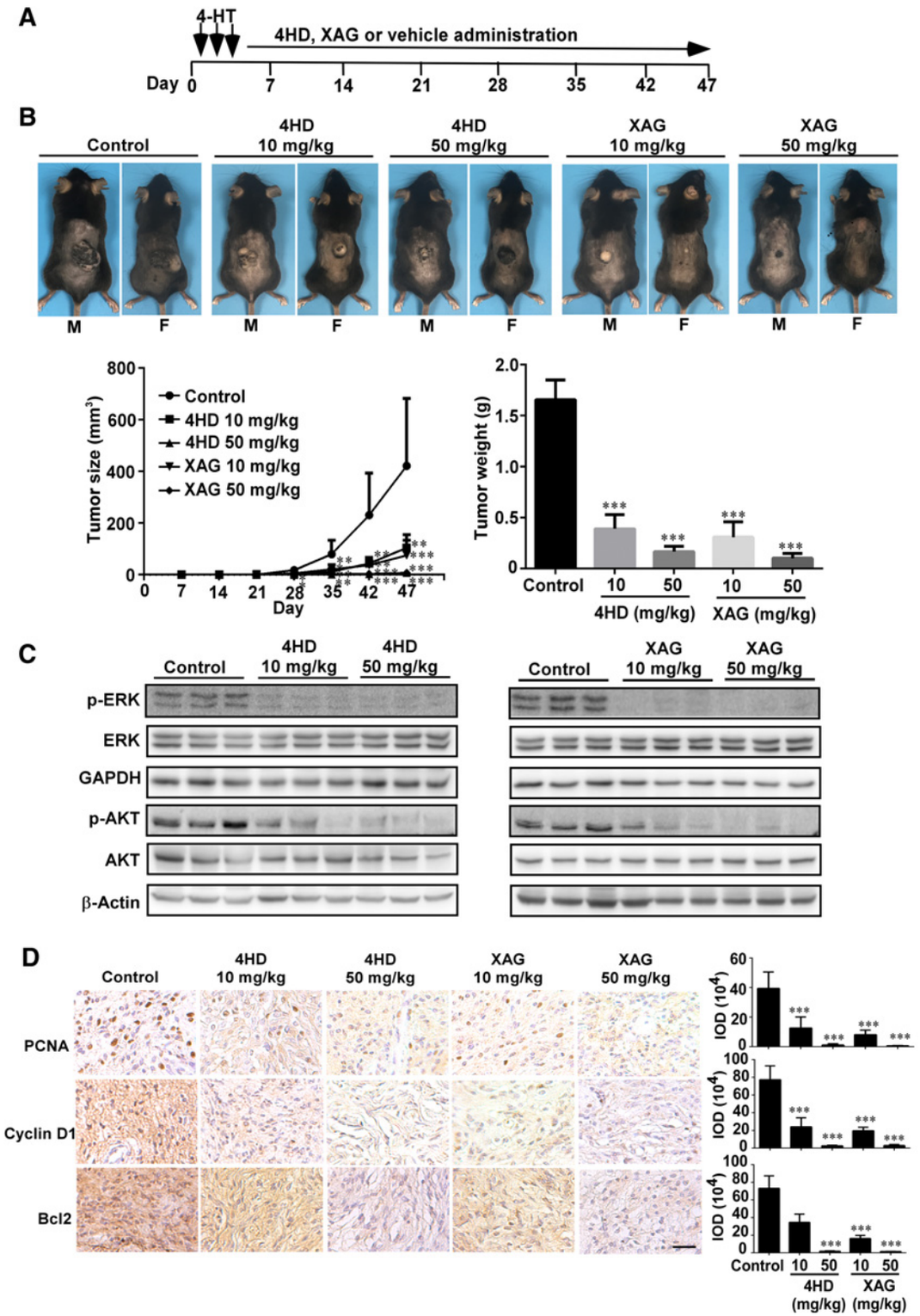

Figure 5.

Prevention of BRAFV600E/PTEN-null induced melanoma by 4HD or XAG. **A,** BRAFV600E/PTEN-null mice (6–8 weeks old) were treated with 2.5 μL of 5 mmol/L 4-HT by local application to the dorsal surface. Mice were randomly assigned to be administered 4HD (10 mg/kg, $n = 10$), 4HD (50 mg/kg, $n = 10$), XAG (10 mg/kg, $n = 10$), XAG (50 mg/kg, $n = 10$), or solvent control ($n = 10$). **B,** Representative images of solvent control, 4HD- or XAG-treated mice immediately after drug administration are shown at day 47. Tumor size in each of the treatment groups was measured every week. Tumor weight was measured at day 47. **C,** Mice were euthanized and melanoma specimens were disrupted and then the expression of p-ERKs, ERKs, GAPDH, p-AKT, and AKT, as well as β-actin was assessed by Western blotting. **D,** Melanoma specimens were prepared for staining to detect PCNA, cyclin D1, or Bcl-2 by IHC. Scale bars, 25 μm. Data are shown as mean values ± SE as determined from three independent experiments and the asterisks indicate a significant decrease compared with vehicle control mice (*, $P < 0.05$; **, $P < 0.01$; ***, $P < 0.001$).

Downloaded from http://aacrjournals.org/cancerpreventionresearch/article-pdf/11/10/607/1730510/607.pdf by guest on 23 May 2025

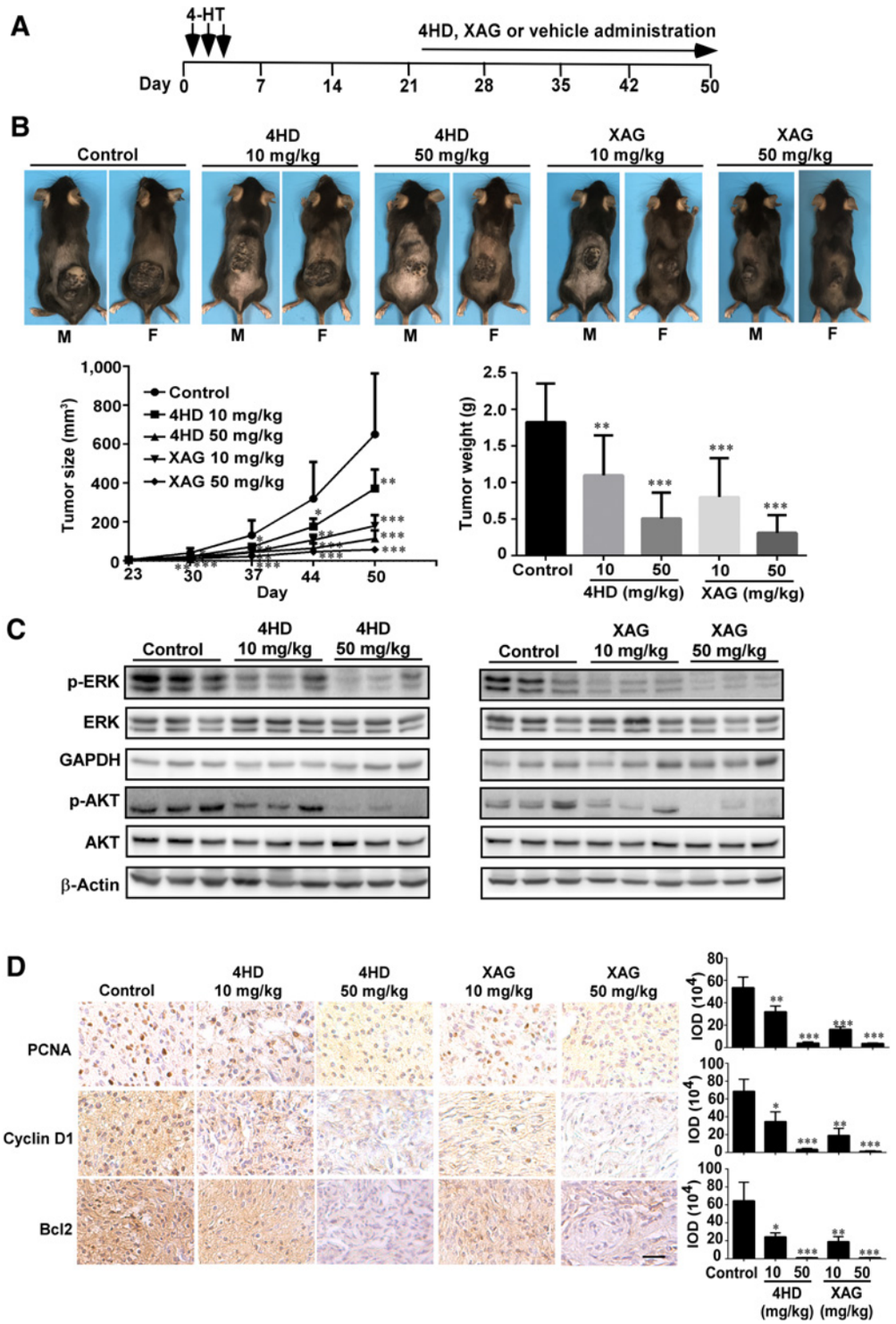

Figure 6.

4HD or XAG suppresses melanoma growth in BRAFV600E/PTEN-null mice. **A,** Melanoma was initiated in BRAFV600E/PTEN-null mice (6–8 weeks old) by local administration of 2.5 μL of 5 mmol/L 4-HT by local injection to the dorsal skin. At 23 days later, when the animals had readily measurable melanoma lesions, mice were randomly divided into 5 groups that were administered 4HD (10 mg/kg, $n = 10$), 4HD (50 mg/kg, $n = 10$), XAG (10 mg/kg, $n = 10$), XAG (50 mg/kg, $n = 10$), or solvent control ($n = 10$). **B,** Representative images of solvent control, 4HD- or XAG-treated mice immediately after drug administration are shown at day 50. Tumor size in each of the treatment groups was measured every week. Tumor weight was measured at day 50. **C,** Mice were euthanized and melanoma specimens were disrupted and then the expression of p-ERKs, ERKs, GAPDH, p-AKT, and AKT as well as β-actin was assessed by Western blotting. **D,** Melanoma specimens were prepared for staining for PCNA, cyclin D1, or Bcl-2 by IHC. Scale bars, 25 μm. Data are represented as mean values ± SE as determined from three independent experiments and the asterisks indicate a significant decrease compared with vehicle control mice (*, $P < 0.05$; **, $P < 0.01$; ***, $P < 0.001$).

Downloaded from http://aacrjournals.org/cancerpreventionresearch/article-pdf/11/10/607/1730510/607.pdf by guest on 23 May 2025

another important pathway driving pathogenesis in BRAF wild-type melanomas as well as for acquired resistance in BRAF-mutant melanomas (27, 28). The lifespan of mice expressing the BRAFV600E mutant combined with *Pten*-loss–activated PI3K is less than 100 days, whereas the lifespan of BRAFV600E-only mutant mice is more than 800 days (17). Currently, several clinical trials examining the combination of PI3K/AKT inhibitors with MAPK pathway inhibitors are ongoing or planned. Moreover, activating point mutations in NRAS occur in up to 20% of melanomas, resulting in constitutive NRAS-mediated signaling and activation of the BRAF/MEK/ERKs and PI3K/AKT signaling cascades. These signaling cascades are prototypic survival pathways that have been implicated in tumorigenesis of NRAS-mutant melanoma (29, 30). Emerging preclinical evidence suggests that the combined targeting of these two pathways with selective small-molecule inhibitors might be effective in treating NRAS-mutant melanomas (11, 29). All this evidence indicates that the inhibitors, 4HD and XAG, target both the BRAF/MEK/ERKs and PI3K/AKT signaling cascades and are promising chemopreventive or potential therapeutic agents against melanomagenesis.

The BRAF/MEK/ERKs and PI3K/AKT signaling cascades interact with each other to mediate cell proliferation and apoptosis, and have been implicated in tumorigenesis of many cancer cell types including melanoma (12, 13, 31, 32). Our results showed that 4HD or XAG directly inhibit BRAFV600E and PI3K activation leading to decreased cyclin D1 expression, which results in G_0–G_1 cell cycle arrest in melanoma cells (Fig. 3). Moreover, these compounds also induced apoptosis in melanoma cells, which was evident by the increased levels of cleaved PARP and caspase-3 and a decrease in Bcl-2 expression levels (Fig. 4), which are considered markers for cells undergoing apoptosis (33, 34). Notably, 4HD and XAG show inhibitory effects in the BRAFV600E/PTEN–null mouse model (Fig. 5 and 6). This mouse model is a well-known mouse model for studying the mechanisms of melanomagenesis and new drug development (35–37). Either 4HD or XAG decreased phosphorylation levels of ERKs and AKT, which are downstream of BRAF and PI3-K. They also decreased levels of the cell proliferation markers PCNA and cyclin D1 and anti-apoptotic Bcl-2 in the *in vivo* studies. These findings provide a rationale for pushing these drugs into rapid clinical translation.

In summary, this study identified 4HD and XAG as novel preventive and therapeutic agents for suppressing melanomagenesis acting by directly targeting both BRAFV600E and PI3K, and could potentially provide a new option for the clinical oral treatment of melanoma.

Disclosure of Potential Conflicts of Interest

No potential conflicts of interest were disclosed.

Authors' Contributions

Conception and design: T. Zhang, N. Oi, Z. Dong
Development of methodology: T. Zhang, Q. Wang, G. Gao, K. Yao
Acquisition of data (provided animals, acquired and managed patients, provided facilities, etc.): T. Zhang, Q. Wang, G. Gao, K. Wang, T. Wang
Analysis and interpretation of data (e.g., statistical analysis, biostatistics, computational analysis): T. Zhang, Q. Wang, G. Gao, H. Chen, K. Yao, X. Chang, A.M. Bode, S.M. Lippman, Z. Dong
Writing, review, and/or revision of the manuscript: T. Zhang, A.M. Bode, S.M. Lippman, Z. Dong
Administrative, technical, or material support (i.e., reporting or organizing data, constructing databases): T. Zhang, Q. Wang, N. Oi, W. Ma, X. Chang, M.-H. Lee, M.G. Rathore, H. Ashida, S.M. Lippman
Study supervision: S.M. Lippman, Z. Dong
Other (extracted, purified, and structurally elucidated XAG and 4HD in this study; contributed to the chemical part in this study): M. Fredimoses
Other (*in vitro* kinase assays): T. Zykova
Other (compounds' extraction and isolation): K. Reddy

Acknowledgments

The authors thank Tara Adams for supporting animal experiments, Todd Schuster for supporting experiments and Dr. Tia Rai for assistance in submitting this manuscript (The Hormel Institute, University of Minnesota, Austin, MN). This work was supported by The Hormel Foundation, NIH grants CA166011, CA187027, and CA196639 (to Z. Dong) and a National Natural Science Foundation of China, "Foreign Young Scientist" grant, NSFC81650110530 (to M. Fredimoses).

The costs of publication of this article were defrayed in part by the payment of page charges. This article must therefore be hereby marked *advertisement* in accordance with 18 U.S.C. Section 1734 solely to indicate this fact.

Received March 15, 2018; revised May 22, 2018; accepted June 27, 2018; published first July 6, 2018.

References

1. Owens B. Melanoma. Nature 2014;515:S109.
2. Miller AJ, Mihm MC. Melanoma. N Engl J Med 2006;355:51–65.
3. Davies H, Bignell GR, Cox C, Stephens P, Edkins S, Clegg S, et al. Mutations of the BRAF gene in human cancer. Nature 2002;417:949–54.
4. Garnett MJ, Marais R. Guilty as charged: B-RAF is a human oncogene. Cancer Cell 2004;6:313–9.
5. Dhomen N, Marais R. BRAF signaling and targeted therapies in melanoma. Hematol Oncol Clin North Am 2009;23:529–45.
6. Holderfield M, Deuker MM, McCormick F, McMahon M. Targeting RAF kinases for cancer therapy: BRAF-mutated melanoma and beyond. Nat Rev Cancer 2014;14:455–67.
7. Lim SY, Menzies AM, Rizos H. Mechanisms and strategies to overcome resistance to molecularly targeted therapy for melanoma. Cancer 2017;123:2118–29.
8. Obaid NM, Bedard K, Huang WY. Strategies for overcoming resistance in tumours harboring BRAF mutations. Int J Mol Sci 2017;18:585.

Downloaded from http://aacrjournals.org/cancerpreventionresearch/article-pdf/11/10/607/1730510/607.pdf by guest on 23 May 2025

9. Niessner H, Schmitz J, Tabatabai G, Schmid AM, Calaminus C, Sinnberg T, et al. PI3K pathway inhibition achieves potent antitumor activity in melanoma brain metastases in vitro and in vivo. Clin Cancer Res 2016;22:5818–28.
10. Touil Y, Zuliani T, Wolowczuk I, Kuranda K, Prochazkova J, Andrieux J, et al. The PI3K/AKT signaling pathway controls the quiescence of the low-Rhodamine123-retention cell compartment enriched for melanoma stem cell activity. Stem Cells 2013;31:641–51.
11. Shimizu T, Tolcher AW, Papadopoulos KP, Beeram M, Rasco DW, Smith LS, et al. The clinical effect of the dual-targeting strategy involving PI3K/AKT/mTOR and RAS/MEK/ERK pathways in patients with advanced cancer. Clin Cancer Res 2012;18:2316–25.
12. Stahl JM, Sharma A, Cheung M, Zimmerman M, Cheng JQ, Bosenberg MW, et al. Deregulated Akt3 activity promotes development of malignant melanoma. Cancer Res 2004;64:7002–10.
13. Madhunapantula SV, Mosca PJ, Robertson GP. The Akt signaling pathway: an emerging therapeutic target in malignant melanoma. Cancer Biol Ther 2011;12:1032–49.
14. Yasuda M, Kawabata K, Miyashita M, Okumura M, Yamamoto N, Takahashi M, et al. Inhibitory effects of 4-hydroxyderricin and xanthoangelol on lipopolysaccharide-induced inflammatory responses in RAW264 macrophages. J Agric Food Chem 2014;62:462–7.
15. Zhang T, Sawada K, Yamamoto N, Ashida H. 4-Hydroxyderricin and xanthoangelol from Ashitaba (Angelica keiskei) suppress differentiation of preadiopocytes to adipocytes via AMPK and MAPK pathways. Mol Nutr Food Res 2013;57:1729–40.
16. Kawabata K, Sawada K, Ikeda K, Fukuda I, Kawasaki K, Yamamoto N, et al. Prenylated chalcones 4-hydroxyderricin and xanthoangelol stimulate glucose uptake in skeletal muscle cells by inducing GLUT4 translocation. Mol Nutr Food Res 2011;55:467–75.
17. Dankort D, Curley DP, Cartlidge RA, Nelson B, Karnezis AN, Damsky WE, Jr., et al. Braf(V600E) cooperates with Pten loss to induce metastatic melanoma. Nat Genet 2009;41:544–52.
18. Schrödinger LLC. QMPolarized Protocol. New York, NY: Schrodinger Suite; 2015.
19. Ahmad N, Feyes DK, Nieminen AL, Agarwal R, Mukhtar H. Green tea constituent epigallocatechin-3-gallate and induction of apoptosis and cell cycle arrest in human carcinoma cells. J Natl Cancer Inst 1997;89:1881–6.
20. Flaherty KT, Puzanov I, Kim KB, Ribas A, McArthur GA, Sosman JA, et al. Inhibition of mutated, activated BRAF in metastatic melanoma. N Engl J Med 2010;363:809–19.
21. Sosman JA, Kim KB, Schuchter L, Gonzalez R, Pavlick AC, Weber JS, et al. Survival in BRAF V600–mutant advanced melanoma treated with vemurafenib. N Engl J Med 2012;366:707–14.
22. Chapman PB, Hauschild A, Robert C, Haanen JB, Ascierto P, Larkin J, et al. Improved survival with vemurafenib in melanoma with BRAF V600E mutation. N Engl J Med 2011;364:2507–16.
23. Kefford R, Arkenau H, Brown MP, Millward M, Infante JR, Long GV, et al. Phase I/II study of GSK2118436, a selective inhibitor of oncogenic mutant BRAF kinase, in patients with metastatic melanoma and other solid tumors. J Clin Oncol 2010;28:8503–.
24. Wagle N, Emery C, Berger MF, Davis MJ, Sawyer A, Pochanard P, et al. Dissecting therapeutic resistance to RAF inhibition in melanoma by tumor genomic profiling. J Clin Oncol 2011;29:3085–96.
25. Larkin J, Ascierto PA, Dreno B, Atkinson V, Liszkay G, Maio M, et al. Combined vemurafenib and cobimetinib in BRAF-mutated melanoma. N Engl J Med 2014;371:1867–76.
26. Long GV, Stroyakovskiy D, Gogas H, Levchenko E, de Braud F, Larkin J, et al. Combined BRAF and MEK inhibition versus BRAF inhibition alone in melanoma. N Engl J Med 2014;371:1877–88.
27. Greger JG, Eastman SD, Zhang V, Bleam MR, Hughes AM, Smitheman KN, et al. Combinations of BRAF, MEK, and PI3K/mTOR inhibitors overcome acquired resistance to the BRAF inhibitor GSK2118436 dabrafenib, mediated by NRAS or MEK mutations. Mol Cancer Ther 2012;11:909–20.
28. Lassen A, Atefi M, Robert L, Wong DJ, Cerniglia M, Comin-Anduix B, et al. Effects of AKT inhibitor therapy in response and resistance to BRAF inhibition in melanoma. Mol Cancer 2014;13:83.
29. Posch C, Moslehi H, Feeney L, Green GA, Ebaee A, Feichtenschlager V, et al. Combined targeting of MEK and PI3K/mTOR effector pathways is necessary to effectively inhibit NRAS mutant melanoma *in vitro* and *in vivo*. PNAS 2013;110:4015–20.
30. Giehl K. Oncogenic Ras in tumour progression and metastasis. Biol Chem 2005;386:193–205.
31. Karasarides M, Chiloeches A, Hayward R, Niculescu-Duvaz D, Scanlon I, Friedlos F, et al. B-RAF is a therapeutic target in melanoma. Oncogene 2004;23:6292–8.
32. McCubrey JA, Steelman LS, Chappell WH, Abrams SL, Wong EW, Chang F, et al. Roles of the Raf/MEK/ERK pathway in cell growth, malignant transformation and drug resistance. Biochim Biophys Acta 2007;1773:1263–84.
33. Baldin V, Lukas J, Marcote MJ, Pagano M, Draetta G. Cyclin D1 is a nuclear protein required for cell cycle progression in G1. Genes Dev 1993;7:812–21.
34. Reed JC. Bcl-2 and the regulation of programmed cell death. J Cell Biol 1994;124:1–6.
35. Xie XQ, Koh JY, Price S, White E, Mehnert JM. Atg7 Overcomes Senescence and Promotes Growth of Braf(V600E)-Driven Melanoma. Cancer Discov 2015;5:410–23.
36. Yuan P, Ito K, Perez-Lorenzo R, Del Guzzo C, Lee JH, Shen C-H, et al. Phenformin enhances the therapeutic benefit of BRAFV600E inhibition in melanoma. Proc Natl Acad Sci U S A 2013;110:18226–31.
37. Olvedy M, Tisserand JC, Luciani F, Boeckx B, Wouters J, Lopez S, et al. Comparative oncogenomics identifies tyrosine kinase FES as a tumor suppressor in melanoma. J Clin Invest 2017;127:2310–25.

Downloaded from http://aacrjournals.org/cancerpreventionresearch/article-pdf/11/10/607/1730510/607.pdf by guest on 23 May 2025

Downloaded from http://aacrjournals.org/cancerpreventionresearch/article-pdf/11/10/607/1730510/607.pdf by guest on 23 May 2025